Preprints of the 21st IFAC World Congress (Virtual)
Berlin, Germany, July 12-17, 2020

Output Feedback Control of Radially-Dependent Reaction-Diffusion PDEs on Balls of Arbitrary Dimensions

Rafael Vazquez * **Jing Zhang** ** **Miroslav Krstic** *** **Jie Qi** **

* *Dept. of Aerospace Engineering, Universidad de Sevilla, Camino de los Descubrimiento s.n., 41092 Sevilla, Spain (e-mail: rvazquez1@us.es).*
** *College of Information Science and Technology, Donghua University, Shanghai 201620 China (e-mails: zhangj0811@163.com and jieqi@dhu.edu.cn).*
*** *Dept. of Mechanical and Aerospace Engineering, University of California San Diego, La Jolla, CA 92093-0411, USA (e-mail: krstic@ucsd.edu).*

Abstract: Recently, the problem of boundary stabilization and estimation for unstable linear constant-coefficient reaction-diffusion equation on n-balls (in particular, disks and spheres) has been solved by means of the backstepping method. However, the extension of this result to spatially-varying coefficients is far from trivial. Some early success has been achieved under simplifying conditions, such as radially-varying reaction coefficients under revolution symmetry, on a disk or a sphere. These particular cases notwithstanding, the problem remains open. The main issue is that the equations become singular in the radius; when applying the backstepping method, the same type of singularity appears in the kernel equations. Traditionally, well-posedness of these equations has been proved by transforming them into integral equations and then applying the method of successive approximations. In this case, with the resulting integral equation becoming singular, successive approximations do not easily apply. This paper takes a different route and directly addresses the kernel equations via a power series approach, finding in the process the required conditions for the radially-varying coefficients and stating the existence of the series solution. This approach provides a direct numerical method that can be readily applied, despite singularities, to both control and observer boundary design problems.

1. INTRODUCTION

In this paper we introduce an explicit boundary output-feedback control law to stabilize an unstable linear *radially-dependent* reaction-diffusion equation on an n-ball (which in 2-D is a disk and in 3-D a sphere).

This paper extends the spherical harmonics [4] approach of [20], which assumed constant coefficients, using some of the ideas of [24]; for the sake of brevity we will mainly show the modifications required with respect to [20], skipping the details when they are identical. For a finite number of harmonics, we design boundary feedback laws and output injection gains using the backstepping method [7] (with kernels computed using a power series approach) which allows us to obtain exponential stability of the origin in the L^2 norm. Higher harmonics will be naturally open-loop stable. The required conditions for the radially-varying coefficients are found in the analysis of the numerical method and are non-obvious (evenness of the reaction coefficient). The idea of using a power series to compute backstepping kernels was first seen in [2] (without much analysis of the method itself, but rather numerically optimizing the approximation) and later in [6], where piecewise-smooth kernels require the use of several series. Here, we state that the method provides a unique solution leaving the question of convergence of the series (i.e., analyticity of the kernel) for future work; the proof of the result is skipped due to page limitation and will be given in an upcoming publication.

Some partial results towards the solution of this problem were obtained in [22] and [21] for the disk and sphere, respectively; however they required simmetry conditions. Older results in this spirit were obtained in [18] and [12].

Previous results and applications in multi-dimensional domains include multi-agent deployment in 3-D space [13] (by combining the ideas of [20] and [10]), convection problem on annular domains [19], PDEs with boundary conditions governed by lower-dimensional PDEs [14, 24], multi-dimensional cuboid domains [11].

The backstepping method has proved itself to be an ubiquitous method for PDE control, with many other applications including, among others, flow control [16, 23], nonlinear PDEs [17], hyperbolic 1-D systems [9, 3, 1], or delays [8]. Nevertheless, other design methods are also applicable to the geometry considered in this paper (see for instance [15] or [5]).

⋆ This work was supported by the National Natural Science Foundation of China (61773112), the Fundamental Research Funds for the Central Universities and Graduate Student Innovation Fund of Donghua University (CUSF-DH-D-2019089) and the scholarship from China Scholarship Council (CSC201806630010). R. Vazquez acknowledges financial support of the Spanish Ministerio de Ciencia, Innovación y Universidades under grant PGC2018-100680-B-C21

Copyright lies with the authors

The structure of the paper is as follows. In Section 2 we introduce the problem. In Section 3 we state our stability result. We state the well-posedness of the kernels in Section 4, but the proof is skipped due to page limitation. We briefly talk about the observer in Section 5, but skip most details based on its duality with respect to the controller. Next we give some simulation results in Section 6. We finally conclude the paper with some remarks in Section 7.

2. N-D REACTION-DIFFUSION SYSTEM ON AN N-BALL

Following [20], a varying coefficient reaction-diffusion system in an n-dimensional ball of radius R can be written in n-dimensional spherical coordinates, also known as ultraspherical coordinates (see [4], p. 93), which consist of one radial coordinate and $n-1$ angular coordinates. Then, using a (complex-valued) Fourier-Laplace series of Spherical Harmonics [1] to handle the angular dependencies, one reaches the following independent complex-valued 1-D reaction-diffusion equation for each harmonic:

$$\partial_t u_l^m = \frac{\epsilon}{r^{n-1}}\partial_r\left(r^{n-1}\partial_r u_l^m\right) - l(l+n-2)\frac{\epsilon}{r^2}u_l^m + \lambda(r)u_l^m, \tag{1}$$

evolving in $r \in [0, R]$, $t > 0$, with boundary conditions

$$u_l^m(t, R) = U_l^m(t), \tag{2}$$

In these equations, we have considered Dirichlet boundary conditions. The measurement would be the flux at the boundary, namely $\partial_r u_l^m(t, R)$.

In the above equations, the integers m and l stand for the order and degree of the harmonic, respectively. Note that the higher the degree (corresponding to high frequencies), the more "naturally" stable (1)–(2) is, as seen next. Define the L^2 norm

$$\|f(r)\|_{L^2}^2 = \int_0^R |f(r)|^2 r^{n-1} dr. \tag{3}$$

and the associated L^2 space as usual, where $|f|^2 = ff^*$, being f^* the complex conjugate of f.

Lemma 1. Given $\lambda(r)$ and R, there exists $L \in \mathbb{N}$ such that, for all $l > L$, the equilibrium $u_l^m \equiv 0$ of system (1)-(2) is open loop exponentially stable, namely, for $U_l^m = 0$ in (1) there exists a positive constant D_1, such that for all t

$$\|u_l^m(t, \cdot)\|_{L^2}^2 \leq e^{-D_1 t}\|u_l^m(0, \cdot)\|_{L^2}^2. \tag{4}$$

D_1 is independent of l, and only depends on n, $\lambda(r)$, ϵ, and R, and can be chosen as large as desired just by increasing the values of L.

The proof is skipped as it mimics [24] just by using the L^2 norm as a Lyapunov function and Poincare's inequality.

Thus one only needs to stabilize the unstable mode with $|l| < L$. Since the different modes are not coupled, it allows us to stabilize them separately and re-assembling them. Moreover since only a finite number of harmonics is stabilized, there is no need to worry about the convergence of the control law as in [20], with its Spherical Harmonics series being just a finite sum.

[1] Spherical harmonics were introduced by Laplace to solve the homonymous equation and have been widely used since, particularly in geodesics, electromagnetism and computer graphics. A very complete treatment on the subject can be found in [4].

Our objective can now be stated as follows. Considering only the unstable modes, design an *output-feedback* control law for U_l^m using, for each mode, only the measurement of $\partial_r u_l^m(t, R)$. Our design procedure is established in the next section along with our main stability result.

3. STABILITY OF CONTROLLED HARMONICS

Next, for the unstable modes we design the output-feedback law. The observer and controller are designed separately using the backstepping method, by following [20]; in this reference it is shown that both the feedback and the output injection gains can be found by solving a certain kernel PDE equation, which is essentially the same for both the controller and the observer. Thus, for the sake of brevity and to avoid repetitive material, we only show how to obtain the (full-state) control law, giving the basic observer design and some additional remarks later in Section 5.

3.1 Design of a full-state feedback control law for unstable modes

Based on the backstepping method [7], our idea is utilizing a invertible Volterra integral transformation

$$w_l^m(t, r) = u_l^m(t, r) - \int_0^r K_{lm}^n(r, \rho)u_l^m(t, \rho)d\rho, \tag{5}$$

where the kernel $K_{lm}^n(r, \rho)$ is to be determined, which defined on the domain $\mathcal{T}_k = \{(r, \rho) \in \mathbb{R}^2; 0 \leq \rho \leq r \leq R\}$ to convert the unstable system (1)-(2) into an exponentially target system:

$$\partial_t w_l^m = \epsilon\frac{\partial_r(r^{n-1}\partial_r w_l^m)}{r^{n-1}} - \epsilon l(l+n-2)\frac{w_l^m}{r^2} - cw_l^m, \tag{6}$$

$$w_l^m(t, R) = 0, \tag{7}$$

where the constant $c > 0$ is an adjustable convergence rate. From (5) and (7), let $r = R$, we obtain the boundary control as the following full-state law

$$U_l^m(t) = \int_0^R K_{lm}^n(R, \rho)u_l^m(t, \rho)d\rho. \tag{8}$$

Following closely the steps of [20] to find conditions for the kernels, and defining $K_{lm}^n(r, \rho) = G_{lm}^n(r, \rho)\rho\left(\frac{\rho}{r}\right)^{l+n-2}$, we finally reach a PDE that the G-kernels need to verify:

$$\frac{\lambda(\rho)+c}{\epsilon}G_{lm}^n = \partial_{rr}G_{lm}^n + (3-n-2l)\frac{\partial_r G_{lm}^n}{r} - \partial_{\rho\rho}G_{lm}^n + (1-n-2l)\frac{\partial_\rho G_{lm}^n}{\rho}, \tag{9}$$

with only one boundary condition:

$$G_{lm}^n(r, r) = -\frac{\int_0^r(\lambda(\sigma)+c)d\sigma}{2r\epsilon}. \tag{10}$$

We assume as usual that these kernel equations are well-posed and the resulting kernel is bounded in $\mathcal{T}$; this will be analyzed later in Section 4, providing a numerical method for its computation.

3.2 Closed-loop stability analysis of unstable modes

To obtain the stability result of closed-loop system, we need three elements. We begin by stating the stability

result for the target system. We follow by obtaining the existence of an inverse transformation that allows us to recover our original variable from the transformed variable. Then we relate the L^2 norm with spherical harmonics. With these elements, we construct the proof of stability mapping the result for the target system to the original system. This is done by showing that the transformation is an invertible map from L^2 into L^2.

We first discuss the stability of the target system, having the following Lemma:

Lemma 2. For all $l \in \mathbb{N}$, and for $c \geq 0$, the equilibrium $w_l^m \equiv 0$ of system (6)–(7) is exponentially stable, i.e., there exists a positive constant D_2 such that for all t,

$$\|w_l^m(t,\cdot)\|_{L^2}^2 \leq e^{-D_2 t}\|w_l^m(0,\cdot)\|_{L^2}^2, \tag{11}$$

where the constant D_2 is independent of n, l or m, and only depends on c, ϵ, and R; it can be chosen as large as desired just by increasing the value of c.

Proof. Consider the Lyapunov function:

$$V_2(t) = \frac{1}{2}\|w_l^m(t,\cdot)\|_{L^2}^2, \tag{12}$$

then, taking its time derivative, we obtain

$$\begin{aligned}\dot{V}_2 &= \int_0^R \frac{\bar{w}_l^m \partial_t w_l^m + w_l^m \partial_t \bar{w}_l^m}{2} r^{n-1} dr \\ &\leq -\left(\frac{\epsilon}{4R^2} + c\right)\|w_l^m\|_{L^2}^2 \end{aligned} \tag{13}$$

choosing

$$c = \frac{D_2}{2} - \frac{\epsilon}{4R^2} \tag{14}$$

we then obtain, independent of the value of n,

$$\dot{V}_2 \leq -D_2 V_2, \tag{15}$$

thus proving the result.

Lemma 3. For $|l| \leq L$, let c be chosen as in Lemma 2, and assume that the kernel $K_{lm}^n(r,\rho)$ is bounded and integrable. The system (1) with boundary control (8) is closed-loop exponentially stable, namely there exists positive constants C and D_2 such that

$$\|u_l^m(t,\cdot)\|_{L^2}^2 \leq Ce^{-D_2 t}\|u_l^m(0,\cdot)\|_{L^2}^2, \tag{16}$$

C and D_2 are independent of m or l, and only depend on n, L, $\lambda(r)$, ϵ and R.

Proof. The proof consists of two parts, one is existence of an inverse transformation, and then showing the equivalence of norms of the variables u_{lm}^n and w_{lm}^n; the result then follows from the stability of the target system.

As shown in [20], when $K_n(r,\rho)$ is bounded and integrable, the map (5) is reversible and its inverse transformation is

$$u_l^m(t,r) = w_l^m(t,r) + \int_0^r L_{lm}^n(r,\rho) w_l^m(t,\rho) d\rho, \tag{17}$$

which is also bounded and integrable. Call now $\bar{K}$ and $\bar{L}$ the maximum of the bounds of the function $\check{K}_{lm}^n$ and $\check{L}_{lm}^n$ for a given n and all $|l| \leq L$ in their respective domains. It is easy to get

$$\|w_l^m(t,\cdot)\|_{L^2}^2 \leq M_1\|u_l^m(t,\cdot)\|_{L^2}^2, \tag{18}$$

$$\|u_l^m(t,\cdot)\|_{L^2}^2 \leq M_2\|w_l^m(t,\cdot)\|_{L^2}^2. \tag{19}$$

where $M_1 = 2 + R^4\bar{K}/(2n)$ and $M_2 = 2 + R^4\bar{L}/(2n)$. Combining then Lemma 2 with the norm equivalence between u_l^m and w_l^m system stated as in (18) and (19), it is easy to obtain

$$\begin{aligned}&\|u_l^m(t,\cdot)\|_{L^2}^2 \leq M_2\|w_l^m(t,\cdot)\|_{L^2}^2 \\ &\leq M_2 e^{-D_2 t}\|w_l^m(0,\cdot)\|_{L^2}^2 \leq M_1 M_2 e^{-D_2 t}\|u_l^m(0,\cdot)\|_{L^2}^2. \end{aligned} \tag{20}$$

Let $C = M_1 M_2$, the result then follows. □

Note that combining Lemmas 1 and 3 and taking $D = \min\{D_1, D_1\}$, we get the following stability result for *all* spherical harmonics and thus the full physical system.

Theorem 4. The equilibrium $u_l^m \equiv 0$ of system (1)-(2) under control law (8) is closed-loop exponentially stable, namely, there exists a positive constant D, such that for all t

$$\|u_l^m(t,\cdot)\|_{L^2}^2 \leq Ce^{-Dt}\|u_l^m(0,\cdot)\|_{L^2}^2. \tag{21}$$

where D can be chosen as large as desired just by increasing the value of L and c in the control design process.

4. WELL-POSEDNESS OF THE KERNEL EQUATIONS

Next, we state a kernell well-posedness result, which was in part implicitly assumed in Theorem 4, also giving the requirements for $\lambda(r)$. This result also provides a numerical method to compute the kernels, which is an alternative to successive approximations which do not work so well in this case (due to the singularities present at the origin; see for instance [22] to see the resulting singular integral equation that needs to be solved).

Theorem 5. Under the assumption that $\lambda(r)$ is an even analytic function in $[0,1]$, then for a given $n > 1$ and all values of $l \in \mathbb{N}$, there is a unique power series solution $G_{lm}^n(r,\rho)$ for (9)–(10), even in its two variables in the domain $\mathcal{T}$. In addition, if $\lambda(r)$ is analytic but not even, then there is no power series solution to (9)–(10) for all $l \in \mathbb{N}$.

Remark 1. The requirement of evenness for $\lambda(r)$ might seem strange at first sight. However, note that $r = \sqrt{x_1^2 + x_2^2 + \ldots + x_n^2}$, therefore in physical space $\lambda(r)$ will be non-smooth unless it is even. Thus, while the kernels might exist for non-even $\lambda(r)$, we cannot expect them to be smooth, which might be indeed problematic for higher-order harmonics; not so much for lower-order, as shown in [22], which only considers the 0-th order harmonic and consequently only requires boundedness of $\lambda(r)$.

The proof of Theorem 5 cannot be given due to page limitation and will appear in a subsequent journal publication. It is based on expressing a solution to (9)–(10) in the form:

$$G_{lm}^n(r,\rho) = \sum_{i=0}^{\infty}\left(\sum_{j=0}^{i} C_{ij} r^j \rho^{i-j}\right), \tag{22}$$

Note that the series in (22) has been written in a way that collects together (in the parenthesis) all the polynomial terms with the same degree.

5. OBSERVER DESIGN

This section designs an observer for (1)-(2) from the measured output $\partial_r u_l^m(t,R)$ as follows:

$$\partial_t \hat{u}_l^m = \epsilon \frac{\partial_r \left(r^{n-1}\partial_r \hat{u}_l^m\right)}{r^{n-1}} - l(l+n-2)\frac{\epsilon}{r^2}\hat{u}_l^m + \lambda(r)\hat{u}_l^m + p_{lm}^n(r)(\partial_r u_l^m(t,R) - \partial_r \hat{u}_l^m(t,R)), \quad (23)$$

with boundary condition

$$\hat{U}_l^m(t) = U_l^m(t). \quad (24)$$

We need to design the output injection gain $p_{lm}^n(r)$. Closely following [20], define the observer error as $\tilde{u} = u - \hat{u}$. The observer error dynamics are given by

$$\frac{\partial \tilde{u}_{lmt}}{\partial t} = \frac{\epsilon}{r^{n-1}}\partial_r\left(r^{n-1}\partial_r \tilde{u}_{lm}\right) - l(l+n-2)\frac{\epsilon}{r^2}\tilde{u}_{lm} + \lambda(r)\tilde{u}_{lm} - p_{lm}^n(r)\partial_r \tilde{u}_{lm}(t,R), \quad (25)$$

with boundary conditions

$$\tilde{u}_{lm}(t,R) = 0. \quad (26)$$

Next we use the backstepping method to find a value of $p_{lm}^n(r)$ that guarantees convergence of $\tilde{u}$ to zero. This ensures that the observer estimates tend to the true state values. Our approach to design $p(r)$ is to seek a mapping that transforms (25) into the following target system

$$\frac{\partial \tilde{w}_{lmt}}{\partial t} = \frac{\epsilon}{r^{n-1}}\partial_r\left(r^{n-1}\partial_r \tilde{w}_{lm}\right) - c\tilde{w}_{lm} - l(l+n-2)\frac{\epsilon}{r^2}\tilde{w}_{lm}, \quad (27)$$

with boundary conditions

$$\tilde{w}_{lm}(t,R) = 0. \quad (28)$$

The transformation is defined as follows:

$$\tilde{u}_{lm}(t,r) = \tilde{w}_{lm}(t,r) - \int_r^R P_{lm}^n(r,\rho)\tilde{w}_{lm}(t,\rho)d\rho, \quad (29)$$

and then $p_{lm}^n(r)$ will be found from transformation kernel as an additional condition.

From [20], one obtains the following PDE that the kernel must verify:

$$\frac{1}{r^{n-1}}\partial_r\left(r^{n-1}\partial_r P_{lm}^n\right) - \partial_\rho\left(\rho^{n-1}\partial_\rho\left(\frac{P_{lm}^n}{\rho^{n-1}}\right)\right) - l(l+n-2)\left(\frac{1}{r^2} - \frac{1}{\rho^2}\right)P_{lm}^n = -\frac{\lambda(r)}{\epsilon}P_{lm}^n \quad (30)$$

In addition we find a value for the output injection gain kernel

$$p_{lm}^n(r) = \epsilon P_{lm}^n(r,R) \quad (31)$$

Also, the following boundary condition has to be verified

$$0 = \lambda(r) + \epsilon\left(\partial_r P_{lm}^n(r,\rho)\right)\Big|_{\rho=r} + \frac{\epsilon}{r^{n-1}}\frac{d}{dr}\left(r^{n-1}P_{lm}^n(r,r)\right) + \epsilon\partial_\rho\left(\frac{P_{lm}^n(r,\rho)}{\rho^{n-1}}\right)\Big|_{\rho=r} r^{n-1}, \quad (32)$$

which can be written as

$$0 = \lambda(r) + \epsilon\partial_r P_{lm}^n(r,r) + \epsilon\frac{d}{dr}\left(P_{lm}^n(r,r)\right) + (n-1)\frac{\epsilon P_{lm}^n(r,r)}{r} + \epsilon\partial_\rho P_{lm}^n(r,r) - (n-1)\frac{\epsilon P_{lm}^n(r,r)}{r}. \quad (33)$$

Following [20], and after some computations, we reach boundary conditions for the kernel equations as follows

$$P_{lm}^n(0,\rho) = 0, \quad \forall l \neq 0 \quad (34)$$

$$P_{lmr}^n(0,\rho) = 0, \quad \forall l \neq 1 \quad (35)$$

$$P_{lm}^n(r,r) = -\frac{\int_0^r \lambda(\sigma)d\sigma}{2\epsilon}. \quad (36)$$

It turns out the observer kernel equation can be transformed into the control kernel equation, therefore obtaining a similar explicit result. For this, define

$$\check{P}_{lm}^n(r,\rho) = \frac{\rho^{n-1}}{r^{n-1}}P_{lm}^n(\rho,r), \quad (37)$$

and it can be verified that the equation now verified by $\check{P}_{lm}^n(r,\rho)$ is exactly the equation verified by $K_{lm}^n(r,\rho)$. Thus $\check{P}_{lm}^n(r,\rho) = K_{lm}^n(r,\rho)$ and we can apply our previous result of Section 4.

The observer error $\tilde{u}$ has the same stability properties derived in Section 3 for the closed-loop system under the full-state control. As in the controller case, only a limited number of modes need to be estimated; namely, those that are not naturally stable by virtue of Lemma 2, this being the main difference with the result given in [20].

Finally, the controller-observer augmented system can be proved closed-loop stable as in [20], using the separation principle given the linearity of the system, with desired convergence rate, and without much modification; we skip the details for lack of space, which requires going up to H^1 stability, as in [20].

6. SIMULATION STUDY

In this section, the simulation experiment on three-dimensional ball (n=3) is taken as an example to illustrate the effectiveness of proposed control. The system with the output-feedback control law is simulated over $0 \leq t \leq 2s$ with the following parameters: $\epsilon = 1, \lambda(r) = 10r^4 + 50r^2 + 50$, $c = 3$. We consider that the system is initially at the random quantity, $u_0 \in [0, 10]$, and the observer's initial condition is set as actual state plus an error of normal distribution with zero mean and $\sigma^2 = 0.5$.

Fig. 1 shows the plots of the polynomial approximation of kernels K_{lm}^3, which is obtained by using (22) up to a cut-off at the p-th powers. The value of K does not depend on m so we omit that sub-index. The value of p is chosen as $p = 15$. Applying Lemma 1, one can obtain L to be 11; however, here to save space, we only show the first six approximate numerical solutions of control gains. As shown in Fig. 1, we find that the K_l becomes increasingly smaller when l increases.

In order to avoid a dramatic increase in the complexity of simulation caused by the high dimension, in our simulations we employ a method also based on spherical harmonics expansions which greatly reduces the error. Thus, we only calculate the harmonics u_{lm} which only need discretization in the radial direction, and then sum a finite number S of harmonics to recover u. When $S > 0$ is a large enough integer, the error caused by the use of a finite number of harmonics is much smaller than the angular discretization error. Thus, the simulation is carried out using the formula

$$u(t,r,\theta_1,\theta_2) = \sum_{l=0}^{l=S}\sum_{m=-l}^{m=l} u_l^m(t,r)Y_{lm}^3(\theta_1,\theta_2) \quad (38)$$

where the spherical harmonics are defined as

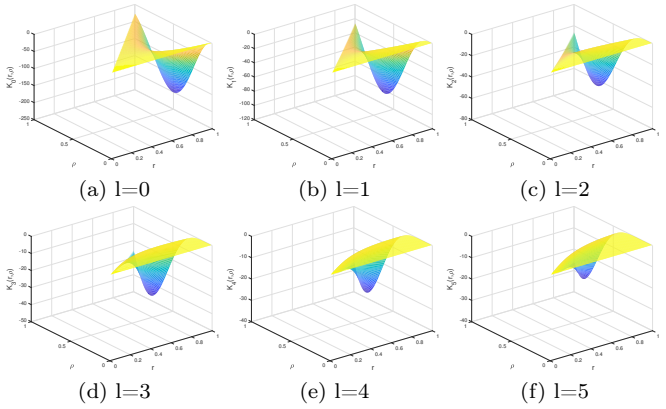

(a) l=0 (b) l=1 (c) l=2

(d) l=3 (e) l=4 (f) l=5

Fig. 1. Polynomial approximation of the first six control gains $K_l(r,\rho)$, $l = 0, 1, \ldots, 5$.

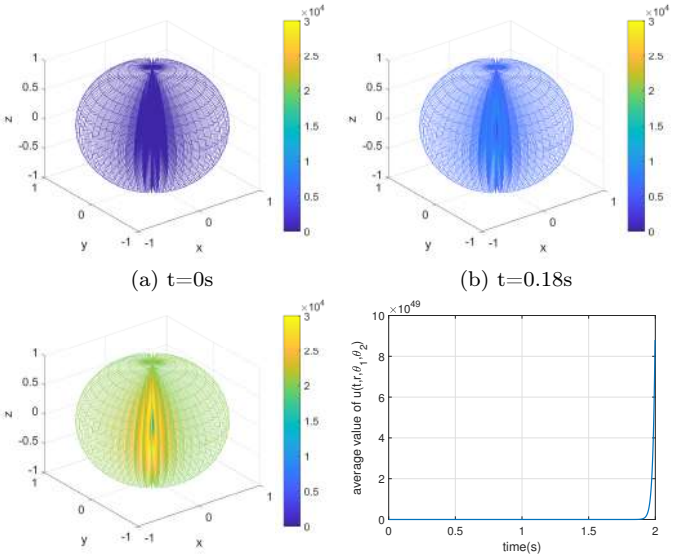

(a) t=0s (b) t=0.18s

(c) t=0.2s (d) Mean of the open-loop system

Fig. 2. Open-loop evolution.

$$Y_{lm}^3(\theta_1,\theta_2) = (-1)^m \sqrt{\frac{2l+1}{4\pi}\frac{(l-m)!}{(l+m)!}} P_{lm}^3(\cos(\theta_1)) e^{jm\theta_2} \tag{39}$$

with P_{lm}^3 the associated Legendre polynomial defined as

$$P_{lm}^3(s) = \frac{1}{2^l l!}(1-s^2)^{m/2}\frac{d^{l+m}}{ds^{l+m}}(s^2-1)^l \tag{40}$$

Fig. 2 and Fig. 3 illustrate the transients of open-loop and closed-loop responses at different times, respectively, where the colour denotes the value of the position at this time. The evolutions of average value of u are plotted in Fig. 2(d) and Fig. 3(e), respectively. (Note that the ranges of color bars are different. And thus avoid the appearance of almost similar colors in fig. 3 of using same upper limit.) Comparing the open-loop and closed-loop evolution, the validity of proposed method is illustrated more intuitively. Fig. 3(f) shows the average of the observation errors, from which it can be found that the system begins to converge to its zero equilibrium after the observation error has already settled to zero as well. The evolutions at different layers, namely $r = 0.002$, $r = 0.3$, $r = 0.5$ and $r = 0.8$, are shown in Fig. 4 (a), (c) , as well as the observer errors are presented in Fig. 4 (b), (d). For clarity, only the first 0.4s of response are shown here. Fig. 5 depicts control effort at

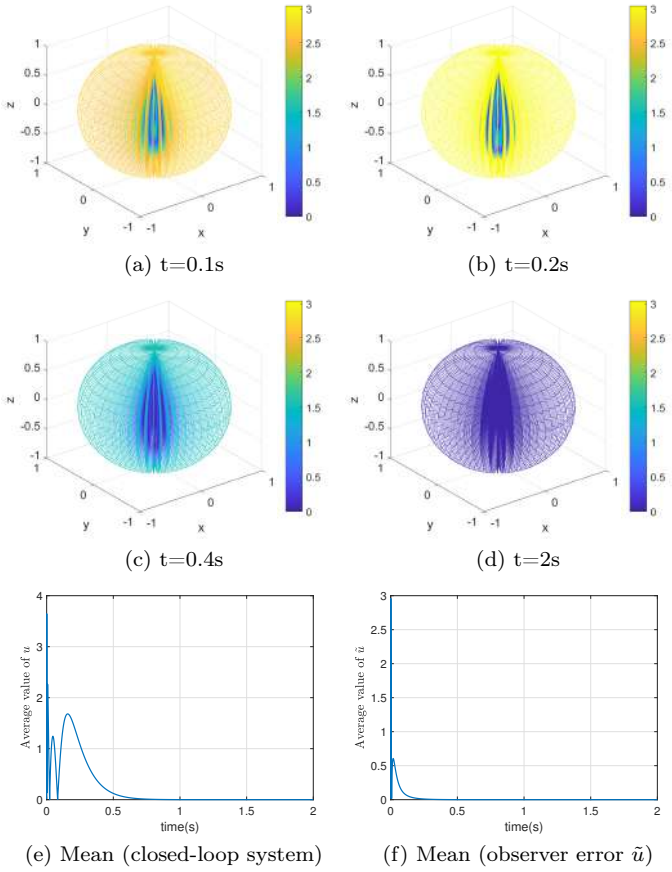

(a) t=0.1s (b) t=0.2s

(c) t=0.4s (d) t=2s

(e) Mean (closed-loop system) (f) Mean (observer error $\tilde{u}$)

Fig. 3. Closed-loop evolution using output feedback control. (a)-(d) Transient states. Note that the different upper ranges of the color bars in Fig. 2 and 3. (e) Mean of system state u. (f) Mean of observer error $\tilde{u}$.

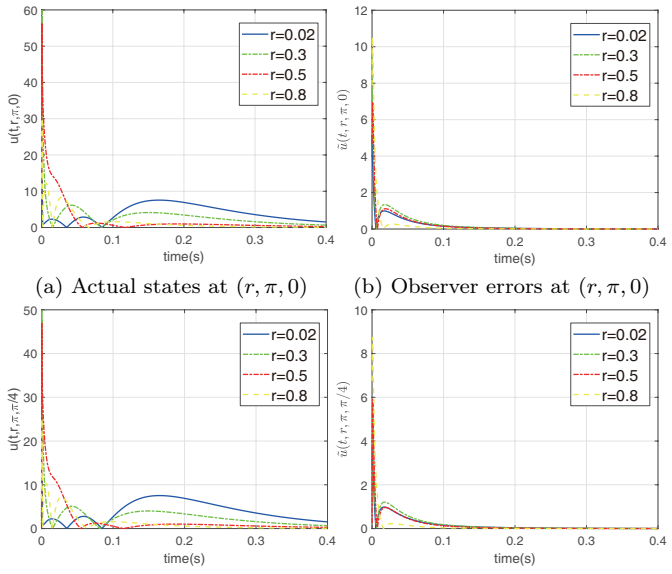

(a) Actual states at $(r,\pi,0)$ (b) Observer errors at $(r,\pi,0)$

(c) Actual states at $(r,\pi,\pi/4)$ (d) Observer errors at $(r,\pi,\pi/4)$

Fig. 4. The details of closed-loop evolution at different r or $\boldsymbol{\theta}$. (a) (c) Actual states. (b) (d) Observer errors between the actual and estimated states.

the boundary. It can be seen that the system driven by the proposed boundary control eventually converges after a short-term fluctuation.

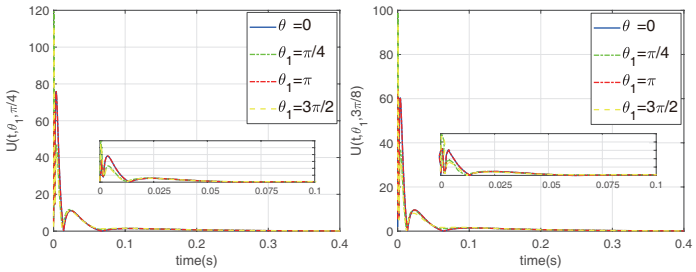

(a) Control effort at $(\theta_1, \pi/4)$ (b) Control effort at $(\theta_1, 3\pi/8)$

Fig. 5. The control effort at different $\boldsymbol{\theta}$.

7. CONCLUSION

We have shown a design to stabilize a radially-varying reaction-diffusion equation on an n-ball, by using an output-feedback boundary control law (with boundary measurements as well) designed through a backstepping method. The radially-varying case proves to be a challenge as the kernel equations become singular in the radius; when applying the backstepping method, the same type of singularity appears in the kernel equations and successive approximations become difficult to use. Using a power series approach, a solution is found, thus providing a numerical method that can be readily applied, to both control and observer boundary design. In addition the required conditions for the radially-varying coefficients are revealed (analyticity and evenness).

In practice, this result can be of interest for deployment of multi-agent systems, by following the spirit of [13]; thus, the radial domain mirrors a radial topology of interconnected agents which follow the reaction-diffusion dynamics to converge to equilibria, that represent different deployment profiles. Since one can choose the plant as desired (thus setting the behaviour of the agents), using analytic reaction coefficients is not actually a restriction, but rather opens the door to richer families of deployment profiles compared with the constant-coefficient case of [13].

On the other hand, the theoretical side of the result needs to be further investigated; besides convergence issues, another avenue of research that can be explored is the relaxation of the analyticity hypothesis by using reaction coefficients belonging to the Gevrey family; the kernels can then be analyzed to verify if they are still analytic, or rather Gevrey-type kernels, or simply do not diverge.

REFERENCES

[1] G. Andrade, R. Vazquez and D. Pagano, "Backstepping stabilization of a linearized ODE-PDE Rijke tube model," *Automatica*, vol. 96, 98-109, 2018.

[2] P. Ascencio, A. Astolfi and T. Parisini, "Backstepping PDE design: A convex optimization approach," *IEEE Transactions on Automatic Control*, vol. 63, pp. 1943–1958, 2018.

[3] J. Auriol and F. Di Meglio, "Minimum time control of heterodirectional linear coupled hyperbolic PDEs," *Automatica*, vol. 71, pp. 300–307, 2016.

[4] K.Atkinson and W. Han, *Spherical Harmonics and Approximations on the Unit Sphere: An Introduction*, Springer, 2012.

[5] V. Barbu, "Boundary stabilization of equilibrium solutions to parabolic equations," *IEEE Transactions on Automatic Control*, vol. 58, pp. 2416–2420, 2013.

[6] L. Camacho-Solorio, R. Vazquez, M. Krstic, "Boundary observers for coupled diffusion-reaction systems with prescribed convergence rate," accepted in *Systems and Control Letters*, 2019.

[7] M. Krstic and A. Smyshlyaev, *Boundary Control of PDEs*, SIAM, 2008

[8] M. Krstic, *Delay Compensation for Nonlinear, Adaptive, and PDE Systems*, Birkhauser, 2009.

[9] L. Hu, R. Vazquez, F. Di Meglio, and M. Krstic, "Boundary exponential stabilization of 1-D inhomogeneous quasilinear hyperbolic systems," *SIAM J. Control Optim.*, vol. 57(2), pp. 963–998, 2019.

[10] T. Meurer and M. Krstic, "Finite-time multi-agent deployment: A nonlinear PDE motion planning approach," *Automatica*, vol. 47, pp. 2534–2542, 2011.

[11] T. Meurer, *Control of Higher-Dimensional PDEs: Flatness and Backstepping Designs*, Springer, 2013.

[12] S.J. Moura, n.A. Chaturvedi, and M. Krstic, "PDE estimation techniques for advanced battery management systems—Part I: SOC estimation," *Proceedings of the 2012 American Control Conference*, 2012.

[13] J. Qi, R. Vazquez and M. Krstic, "Multi-Agent deployment in 3-D via PDE control," *IEEE Transactions on Automatic Control*, vol. 60 (4), pp. 891–906, 2015.

[14] J. Qi, M. Krstic and S. Wang, "Stabilization of reaction-diffusion PDE distributed actuation and input delay," *Proceedings of the 2018 IEEE Conference on Decision and Control (CDC)*, 2018.

[15] R. Triggiani, "Boundary feedback stabilization of parabolic equations.*Appl. Math. Optimiz.*, vol. 6, pp. 201–220, 1980.

[16] R. Vazquez and M. Krstic, *Control of Turbulent and Magnetohydrodynamic Channel Flow*. Birkhauser, 2008.

[17] R. Vazquez and M. Krstic, "Control of 1-D parabolic PDEs with Volterra nonlinearities — Part I: Design," *Automatica*, vol. 44, pp. 2778–2790, 2008.

[18] F. Bribiesca Argomedo, C. Prieur, E. Witrant, and S. Bremond, "A strict control Lyapunov function for a diffusion equation with time-varying distributed coefficients," *IEEE Trans. Autom. Control*, vol. 58, pp. 290–303, 2013.

[19] R. Vazquez and M. Krstic, "Boundary observer for output-feedback stabilization of thermal convection loop," *IEEE Trans. Control Syst. Technol.*, vol.18, pp. 789–797, 2010.

[20] R. Vazquez and M. Krstic, "Boundary control of reaction-diffusion PDEs on balls in spaces of arbitrary dimensions," *ESAIM:Control, Optimization and Calculus of Variations*, vol. 22, No. 4, pp. 1078–1096, 2016.

[21] R. Vazquez and M. Krstic, "Boundary control and estimation of reaction-diffusion equations on the sphere under revolution symmetry conditions," *International Journal of Control*, vol. 92(1), pp. 2–11, 2019.

[22] R. Vazquez and M. Krstic, "Boundary control of a singular reaction-diffusion equation on a disk," *CPDE 2016 (2nd IFAC Workshop on Control of Systems Governed by Partial Differential Equations)*, 2016.

[23] R. Vazquez, E. Trelat and J.-M. Coron, "Control for fast and stable laminar-to-high-Reynolds-numbers transfer in a 2D navier-Stokes channel flow," *Disc. Cont. Dyn. Syst. Ser. B*, vol. 10, pp. 925–956, 2008.

[24] R. Vazquez, M. Krstic, J. Zhang and J. Qi, "Stabilization of a 2-D reaction-diffusion equation with a coupled PDE evolving on its boundary," *Proceedings of the 2019 IEEE Conference on Decision and Control (CDC)*, 2019.